

environment. It is NP-hard to solve optimally and is a core problem in many applications that may involve thousands of agents, such as warehouse automation and traffic management, where balancing solution quality and speed is crucial. Recently, Li et al. (2022) introduced LNS2, a large neighborhood search-based MAPF algorithm that iteratively reuse/fix currently infeasible paths via local re-planning, differing from mainstream MAPF algorithms that rely on more expensive search/backtracking. LNS2 exhibits greater scalability than systematic search planners Sharon et al. (2015) and higher solution quality than priority-based algorithms Erdmann & Lozano-Perez (1987). LNS2 first quickly generates an initial solution that may contain collisions, and then iteratively replans for carefully selected subsets of agents, using a fast, priority-based low-level planner (Safe Interval Path Planning with Soft Constraints (SIPPS) Li et al. (2022) for single agent pathfinding), to finally yield a collision-free solution. However, in high-agent-density tasks, the paths generated by this priority-based planner still often contain a large number of collisions, inevitably increasing the cumulative time needed to address the overall MAPF problem. In parallel to these developments, recent years have seen the development of many (slower) MAPF planners based on Multi-Agent Reinforcement Learning (MARL), which exhibit enhanced cooperation compared to priority-based planners. However, MARL-based planners inevitably exhibit performance degradation when deviating from their training setup (usually only 8 agents), which limits their performance on tasks containing a high density of agents. Moreover, the one-shot Success Rate (SR) of MARL-based planners often drops sharply due to a few agents failing to reach their goals within the time(step) limit, thereby wasting high-quality paths for the majority that succeeded.

In this paper, we propose to combine large neighborhood search and MARL, and introduce a new algorithm called LNS2+RL. Our approach aims to balance the drawbacks of both LNS2 and MARL-based planners, showcasing enhanced performance across diverse scenarios. The overall framework of LNS2+RL follows that of LNS2, iteratively updating the overall solution with re-planned paths. However, it replaces the priority-based planner with a MARL-based planner during the challenging early stages of iterative re-planning to further improve solution quality (i.e., reduce collisions). Our MARL-based planner allows agents to access and reason about historical and predictive information, progressively mastering cooperative decision-making through a carefully crafted curriculum learning strategy. There, we rely on SIPPS to fix the paths planned by agents unable to reach their goals within a limited number of timesteps, thus ensuring the completeness of our MARL-based planner and maximizing the utilization of existing high-quality paths. LNS2+RL then adaptively switches to the original priority-based planner (according to the relative solution quality of the two algorithms in the previous re-planning step), to swiftly clean up remaining collisions, thus naturally trading-off solution quality and re-planning speed. Moreover, since the number of agents involved in each re-planning task (i.e., neighborhood size) is fixed to 8, LNS2+RL can naturally scale the overall planning to thousands of agents while keeping encountered tasks close to MARL’s training distribution.

We tested LNS2+RL on an extensive set of high-difficulty tasks with various team sizes, world sizes, and map structures. Our results indicate LNS2+RL consistently outperforms LNS2 in SR across nearly all tasks, maintaining a comparable Sum of Costs (SoC), and notably reducing the number of remaining Collision Pairs (CP) in the overall solution. Additionally, LNS2+RL surpasses EECBS Li et al. (2021) in SR across all tasks. Compared to LaCAM Okumura (2023), LNS2+RL exhibits a substantial advantage in SR on highly structured maps (achieving 100% SR compared to LaCAM’s 0%), while also achieving significantly lower SoC on less structured maps. Finally, as shown in Figure 1, we experimentally validated our planner in a hybrid simulation of a warehouse environment under real-world conditions, where we let a team of 100 agents (10 real-world, and 90 simulated ones) track the paths obtained by LNS2+RL, using an online execution framework Hönig et al. (2019).

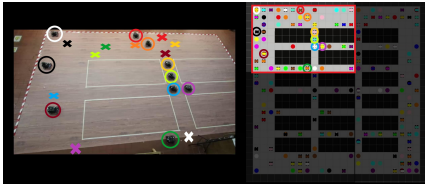


Figure 1: Real portion of the warehouse with 10 robots (left), and complete rviz visualization with 100 robots (right). Real robots are circled in different colors (both in the real and simulated views), and crosses of the same colors represent their goal positions.

2 Prior work

MAPF algorithms developed in recent decades fall into three main categories based on solution optimality: optimal, bounded-suboptimal and unbounded-suboptimal. Common optimal algorithms

include Conflict-Based Search (CBS) Sharon et al. (2015), joint-state A*, and their variants with additional speed-up techniques such as ICBS Boyarski et al. (2015), M* Wagner & Choset (2011), EPEA* Goldenberg et al. (2014), among others. Bounded-suboptimal algorithms trade off solution quality and runtime by finding a solution whose cost is at most w times the optimal cost, where w is a user-specified suboptimality factor. Such MAPF algorithms are usually variants of optimal MAPF algorithms, including EECBS Li et al. (2021), weighted EPEA* Barer et al. (2014), and inflated M* Wagner & Choset (2015), etc. Both optimal and bounded-suboptimal algorithms are able to ensure high solution quality but face scalability challenges when handling thousands of agents, often encountering timeouts or memory overflows. Conversely, unbounded-suboptimal algorithms (such as priority Erdmann & Lozano-Perez (1987) and rule-based planning Luna & Bekris (2011)) prioritize speed over optimality, scaling to thousands of agents easily, but may yield substantially suboptimal solutions in complex tasks and often do not guarantee completeness. More recently, learning-based approaches have begun to emerge. One class of approaches, exemplified by PRIMAL Sartoretti et al. (2019), directly learns a MAPF planner using MARL Ma et al. (2021); Wang et al. (2020), while another combines conventional algorithms with learning, exemplified by switching between two types of algorithms based on certain conditions Skrynnik et al. (2023) or by enhancing conventional algorithms’ components with learned strategies Huang et al. (2022).

3 Background

3.1 Multi-agent path finding

In this paper, we consider a common formulation of the MAPF problem, defined within a 2d 4-edge grid $G = (V, E)$, encompassing a set of m agents $A = \{a_1, \dots, a_m\}$ and a finite set of static obstacles. Each agent a_i initiates from a distinct starting position $s_i \in V$, with the objective of reaching its designated goal $g_i \in V$. At each discretized timestep, an agent can either move to an adjacent vertex or wait at its current vertex. The *path* p_i for each agent is a sequence of adjacent or identical vertices (v_1^i, \dots, v_k^i) satisfying $v_1^i = s_i, v_k^i = g_i$. We assume that the agents wait at their goal vertices until all agents have reached their goals. A *solution* of MAPF $P = \{p_i \mid a_i \in A\}$ is a path set for all agents, ensuring all agents reach their goals at a certain timestep without any vertex (agents occupy the same vertex) or swapping collisions (agents traverse the same edge simultaneously). This paper evaluates solution quality using a *sum of costs* metric, defined as the sum of timesteps required by each agent to reach its goal $\sum_{1 \leq i \leq m} |p_i|$.

3.2 LNS2

LNS2 is an unbounded-suboptimal and memory-efficient MAPF algorithm based on large neighborhood search. It begins by planning a set of paths that may contain collisions, iteratively selecting subsets for re-planning through an Adaptive Large Neighborhood Selection (ALNS) method based on previous experience. A replanning solver then computes new paths for these selected agents and evaluates whether to adopt the new paths depending on whether they reduce or maintain the number of CP within the overall solution. This replanning process continues iteratively until the overall path set is collision-free or the time limit is exceeded.

The low-level, re-planning solver employed in LNS2 is a variant of priority planning (termed PP+SIPPS), which utilizes SIPPS algorithm to plan individual paths for agents in a random priority order. SIPPS aims to find a path for an agent to avoid collisions with hard obstacles (static obstacles) while minimizing collisions with soft obstacles (pre-existing paths). It runs five times faster than Space-Time A*, ensuring completeness and returning the shortest path with zero soft collisions if one exists. However, in dense-obstacle scenarios, SIPPS may produce a path with significantly more soft collisions than the minimum due to its heuristic function ignoring soft collisions that occur when the agent waits within a safe interval that contains soft obstacles. Despite the fast speed of SIPPS, this reduced solution quality necessitates a higher number of iterations to fully solve high-difficulty MAPF instances, resulting in substantial cumulative time expenditure. Therefore, there is an urgent need to develop a new re-planning solver that can generate high-quality solutions (fewer collisions) while potentially sacrificing speed, to find a better balance between quality and time throughout the overall planning.

4 Re-planning tasks as a MARL problem

4.1 Path finding with mixed dynamic obstacles

The re-planning task can be defined as the Path Finding with Mixed Dynamic Obstacles (PMDO) problem. In the PMDO problem, two finite sets of obstacles are considered. The first category, hard obstacles, aligns with the immovable obstacles in conventional MAPF. The second category, soft obstacles, refers to other unselected agents and is characterized by the ability to move to any vertex not occupied by hard obstacles and remain there for an arbitrary duration. Notably, the complete trajectory of each soft obstacle is fully disclosed and remains constant throughout the re-planning task. Any occupied vertex at a given timestep t can contain either a single hard obstacle or multiple soft obstacles/agents. The objective of the re-planning task is to find the shortest path for each selected agent from their start vertex to the goal vertex while avoiding collisions with hard obstacles and minimizing collisions with both soft obstacles and other agents.

4.2 RL environment setup

Aligned with previously outlined MAPF and PMDO problems, we consider a discrete 2D 4-connected gridworld environment where the size of each agent, goal, and obstacle is one grid cell. Each agent can take a discrete action at every timestep, which includes moving one unit towards any of the four cardinal directions or staying still. The agents’ actions are executed synchronously, with collision checks conducted subsequently to the execution of all actions. Actions resulting in collisions with hard obstacles or exceeding world boundaries are classified as invalid. Only valid actions are sampled during training and evaluation, and an additional supervised loss is added to the overall MARL loss.

We initially establish a MAPF task comprising m agents, assigning each a unique start and a corresponding goal position. Using PP+SIPPS to compute the initial path set P for the m agents. Subsequently, a subset of agents is selected, and during the training phase of the MARL model, we keep the subset size n (i.e., the neighborhood size) to 8. The PMDO re-planning task is then formulated by designating the chosen subset as the controlled agents of the MARL model, while the remaining agents act as soft obstacles. A training episode terminates either when all agents are on goal at the end of a timestep (the timestep is higher than the maximum length of the soft obstacle trajectories) or when the episode reaches the pre-defined timestep limit.

4.3 Observation and reward

Aligned with previous works Sartoretti et al. (2019), the environment is partially observable, restricting each agent to only access information within its self-centered field of view (FoV). This assumption enables the trained policy to scale to arbitrary world sizes while fixing the input dimensions of the neural network. The FoV contains global spatial and temporal information derived from the complete map structure and past/predicted trajectories of all soft obstacles and other agents.

Each agent’s current observation at timestep t is divided into two parts. Here, we take agent i as an example. The first part of the observation consists of thirty-one 2D matrices. Following methodologies from previous research Wang et al. (2023), where four matrices represent the actual/projected positions of hard obstacles, other agents, observable agents’ goals, and agent i ’s own goal. Additionally, there are four binary matrices representing the shortest paths of agent i , calculated by the Dijkstra algorithm without considering other agents and soft obstacles. Another map that helps guide agent i closer to its goal is the *SIPPS map*, which represents all vertices traversed by agent i ’s SIPPS path \hat{p}_i (computed only at the beginning of the re-planning task) during $t - 15$ to $t + 15$. To motivate MARL agents to refer to the SIPPS paths while allowing necessary detours to avoid collisions, we introduce an off-route penalty ro , that is

$$ro_t^i = -\alpha \min \|v_t^i - v\|_2, v \in \{(\hat{p}_i)_j \mid t - 15 \leq j < t + 15\}, \quad (1)$$

where α is a predefined hyperparameter, v_t^i is the position of agent i at timestep t , v represents all vertices contained in the SIPPS map of agent i .

To avoid collisions with hard and soft obstacles, we further introduce an *occupancy duration map*, a *blank duration map*, *future trajectory maps*, and *predicted trajectory maps*. The occupancy duration map denotes the ratio of time a vertex will be occupied by obstacles to the predefined episode length, while the blank duration map reflects the ratio of time a vertex will remain obstacle-free. The future

Table 1: Reward structure

Action	Move/Stay (not on goal)	Stay (on goal)	Exceed the maximum length of \hat{P}	Return	Collision with obstacles	Avoid congestion	Off-route
Reward	[-0.4,-0.5,-0.6]	0.0	-0.2	-0.4	-1.5	detailed in equation 2	detailed in equation 1

trajectory maps, comprising nine matrices, represent the positions of soft obstacles from t to $t + 8$. The future trajectories of other agents are crucial to enhancing cooperation, but these trajectories are unknown in advance. Hence, we employ a straightforward yet efficient method for forecasting them. To predict the future trajectory of agent j , we first compute the spatial Euclidean distance between v_t^j and all vertices on \hat{p}_j , and then determine the temporal distance as the absolute difference between t and the timesteps of vertices on \hat{p}_j . The predicted position of agent j at $t + 1$ is then derived from a weighted sum of these spatial and temporal distances, with coefficients of 0.9 for spatial and 0.1 for temporal distances. If the vertex with the minimal sum distance is reachable in one action from v_t^j , it is considered the predicted position for $t + 1$; otherwise, agent j is assumed to remain stationary, with its actual position v_t^j as the predicted position for $t + 1$. The subsequent four vertices on the SIPPS path of the vertex with the minimal sum distance are designated as predicted positions from $t + 2$ to $t + 5$.

In path planning tasks involving a large number of agents, congestion often arises in bottleneck areas of the map, where all agents attempt to traverse the same set of vertices, leading to under-utilization of other vertices and significantly increased collision risks. To alleviate congestion, we introduce the *vertex utilization map* and the *edge utilization maps*, which visualize congestion and assist agents in identifying and avoiding high-density areas, promoting more evenly dispersed paths. Specifically, denote $U(v, t - \beta_l, t + \beta_h)$ and $U((v_1, v_2), t - \beta_l, t + \beta_h)$ as the usage of vertex v and edge (v_1, v_2) during the time period from $t - \beta_l$ to $t + \beta_h$, respectively. They are the sum of the number of times the soft obstacles traverse through the vertex/edge from $t - \beta_l$ to $t + \beta_h$, and the number of times agents traverse through the vertex/edge from $t - \beta_l$ to t . In our experiments, we set β_l to 2 and β_h to 15. The normalized value $\delta \frac{U(v, t - \beta_l, t + \beta_h)}{m}$ and $\delta \frac{U((v_1, v_2), t - \beta_l, t + \beta_h)}{m}$ are then used as the value of each grid in the vertex utilization map and four edge utilization maps ($\delta = 10$). Moreover, we further encourage agents to avoid these congested areas by giving them a small penalty rc calculated by

$$rc_t^i = \delta(\delta_v \frac{U(v, t - \beta_l, t + \beta_h)}{m} + \delta_e \frac{U((v_1, v_2), t - \beta_l, t + \beta_h)}{m}). \quad (2)$$

Here $\delta_v = 0.225$, $\delta_e = 0.075$ are used to balance between vertex and edge information.

The second part of the observation is an eight-element vector consisting of the normalized distance between v_t^i and g_i along the x-axis and y-axis, as well as the total Euclidean distance, the ratio of the number of CP in path planned by the MARL-planner compared to these in \hat{p}_i , the ratio of t to the predefined episode length, the ratio of t to the maximum length of \hat{P} , the ratio of agents who have reached goal, and agent i 's action at $t - 1$.

Our reward structure is shown in Table 1. To expedite task completion, agents currently off-goal are penalized at each step, with its magnitude scaling up according to the task's difficulty within the curriculum learning framework (refer Section 4.5 for details). Agents receive an extra penalty if the current timestep exceeds the maximum length of \hat{P} . Additionally, to foster exploration and learn effective policies, agents are penalized for revisiting their previous timestep's location. Furthermore, we employ reward shaping based on the distance from the goal to guide learning while preserving the invariance of the optimal policy Ng et al. (1999).

4.4 Network structure

Figure 2 illustrates the network architecture of our MARL model, encompassing three primary components: memory encoder, observation encoder, and output heads. Given our assumption of a homogeneous team, we rely on weight sharing across all agents, enabling the model to scale effectively with the number of agents during evaluation.

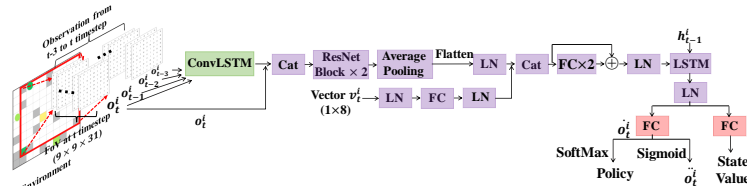


Figure 2: Network structure. Green, purple, and red modules represent the memory encoder, observation encoder, and output heads, respectively. h_{t-1}^i represents the hidden state output by the LSTM unit at the previous time step.

Understanding the underlying dynamics of the environment is crucial in PMDO tasks. Therefore, in addition to utilizing occupied duration map, blank duration map, future trajectory maps, and predicted trajectory maps to capture future temporal information, we incorporate observations from the past three time steps as input to the neural network to provide a more comprehensive understanding of how the environment changes over time. The aggregated observation first passes through a Convolutional Long Short-Term Memory (ConvLSTM) Shi et al. (2015) unit capable of capturing spatial and temporal relationships and then concatenates (Cat) its last hidden state with the current observation o_t^i . The concatenated data then goes through an observation encoder with two ResNet blocks He et al. (2016), followed by an average pooling and Layer Normalization (LN) to produce a one-dimensional feature vector. In parallel, the eight-element vector v_t^i is processed through a Fully Connected (FC) layer, accompanied by two LN. The processed inputs are then concatenated and passed through two FC layers equipped with a residual shortcut, followed by a LN, and ultimately fed into a Long Short-Term Memory (LSTM) cell. The LSTM’s output is further processed by a FC layer, producing a vector \hat{o}_t^i for imitation learning. Subsequently, \hat{o}_t^i passes through a softmax activation to derive the agent’s policy and a sigmoid activation to yield a vector $\hat{\delta}_t^i$ for supervised invalid action loss. Another FC layer also utilizes the LSTM’s output as input to generate the predicted state value.

4.5 Training

Our MARL model is trained by Proximal Policy Optimization (PPO) Schulman et al. (2017). The total loss of the MARL model is $L_{final} = \omega_v \cdot L_v + \omega_\pi \cdot L_\pi + \omega_{invalid} \cdot L_{invalid} - \omega_e \cdot L_e$, where L_v and L_π are the standard critic and actor loss in PPO. L_e is the entropy of the agent’s policy, suppressing its decline shown to encourage exploration and inhibit premature convergence. $L_{invalid}$ is a binary cross-entropy loss (supervised invalid action loss) designed to reduce the logarithmic likelihood of selecting an invalid action. ω_v , ω_π , $\omega_{invalid}$, and ω_e are all manually set hyperparameters.

The training of the MARL model is divided into two stages. As described in Section 4.2, both stages commence by generating a high-level MAPF task and obtaining the initial path set P through PP+SIPPS. Subsequently, a series of PMDO re-planning tasks are generated in different manners and used to train the MARL model. To enhance the agents’ generalization ability, we expose them to diverse scenarios during training by uniformly sampling the world size, hard obstacle rate, and the total number of agents for the MAPF task from a variety of values.

In the first training stage, when constructing each PMDO task, the MARL-controlled agents are chosen randomly, bypassing ALNS. After a MARL episode ends, the path set P is updated with the SIPPS paths \hat{P} calculated at the beginning of the episode, regardless of whether these new paths reduce CP in P . PMDO re-planning tasks are continually generated and only switch to the next new high-level MAPF task when the the maximum iteration limit is reached. Curriculum learning Bengio et al. (2009) is adopted during the first stage of training, allowing agents to rapidly acquire fundamental skills from simpler tasks before progressively facing more challenging scenarios. Specifically, we increase the task difficulty by increasing the hard obstacles rate and the total number of agents in the high-level MAPF tasks and advancing to greater difficulties once the predetermined volume of training data is accumulated. As task difficulty increases, the advantage of SIPPS weakens, and the agents’ preference for safely wandering in a certain area increases. Therefore, we gradually lower the value of α in the off-route penalty to reduce references to SIPPS paths and gradually increase the action cost to incentivize agents to move toward their goal. Additionally, we employ imitation learning (behavior cloning based on the centralized planner ODrM*) at the beginning of each task difficulty in the first stage to explore high-quality regions of the agents’ state-action space.

Upon reaching the manually predefined number of training steps, the training transitions to the second stage. This stage aims to acclimate the MARL policy to scenarios it will face when inserted into the LNS2+RL algorithm. Therefore, both the selection of MARL-controlled agents and the method for updating path set P are exactly the same as the LNS2+RL algorithm’s execution (refer to Section 5 for specifics). A new high-level MAPF task is generated either when P achieves a collision-free state or upon hitting the maximum iteration limit.

5 LNS2+RL

The strengths and weaknesses of PP+SIPPS and the MARL-based planner are distinct yet complementary. PP+SIPPS is fast and effective for simple tasks but tends to generate paths with more

Algorithm 1 LNS2+RL

```

Input: A MAPF instance  $I$ 
 $P = \{p_i \mid a_i \in A\} \leftarrow \text{runInitialSolver}(I)$ 
 $\forall w_h \in W, w_h = 1$ ; build collision graph  $G_c = (V_c, E_c)$ ;  $Q = \emptyset$  and  $|Q| \leq \mu$ 
 $t_m = \max\{|p_i| : p_i \in P\}$ ,  $t_l = d_l \cdot t_m$ ,  $t_h = d_h \cdot t_m$ 
while runtime limit not exceeded and  $CP(P) > 0$  do
   $h \leftarrow \text{selectDestroyHeuristic}(W)$ 
   $A_s, P^- \leftarrow \text{selectAgentSet}(h, I, P, G_c)$ 
  if  $|Q| < \mu$  or  $Q > \rho$  then
     $P^{rl}, \hat{P} \leftarrow \text{runMARLPlanner}(I, P \setminus P^-, A_s, t_l)$ ;  $A_r \leftarrow \{a_i \in A_s : p_{i,\text{end}}^{rl} \neq g_i\}$ 
     $P^{rl} \leftarrow \text{runPriorityPlanner}(I, P \setminus P^-, P^{rl}, A_r, t_l)$ ;  $A_h \leftarrow \{a_i \in A_s : |p_i^{rl}| \geq t_h\}$ 
     $P^{rl} \leftarrow \text{runPriorityPlanner}(I, P \setminus P^-, P^{rl}, A_h, 0)$ 
    Update  $Q$  according to if  $CP(P^{rl}) \geq CP(\hat{P})$ 
    if  $CP((P \setminus P^-) \cup P^{rl}) \leq CP(P)$  then
       $P \leftarrow (P \setminus P^-) \cup P^{rl}$ 
      Update the collision graph  $G_c$ 
      Update  $w_h$ 
      continue
    end if
  else
     $\hat{P} \leftarrow \text{runPriorityPlanner}(I, P \setminus P^-, \emptyset, A_s, 0)$ 
  end if
  if  $CP((P \setminus P^-) \cup \hat{P}) \leq CP(P)$  then
     $P \leftarrow (P \setminus P^-) \cup \hat{P}$ 
    Update the collision graph  $G_c$ 
  end if
  Update  $w_h$ 
end while
return  $P$ 

```

soft collisions in complex tasks. Conversely, our MARL-based planner, although slower, excels at planning paths with fewer collisions in difficult tasks. Therefore, our LNS2+RL algorithm retains the overarching framework of LNS2 but uses the MARL-based planner in the initial, more challenging stages of iterative planning for better solution quality (fewer collisions). It then adaptively switches to PP+SIPPS to quickly clean up the remaining collisions, thus balancing solution quality with the speed of the re-planning task solvers. Moreover, the key limitation in the one-shot SR of MARL-based planners is that while most agents have found high-quality paths, a few fail to reach their goals within the constrained episode length. To address this, we employ PP+SIPPS to supplement paths for these few agents, ensuring the high quality and completeness of the final solution.

The pseudocode for the LNS2+RL algorithm is presented in Algorithm 1. Specifically, for solving a MAPF instance I , LNS2+RL starts by invoking the initial solver (PP+SIPPS) to generate a path set P containing collisions (lines 2), initializing the weights W for the three neighborhood selection methods, and constructing the collision graph G_c (lines 3). Furthermore, LNS2+RL introduces a queue Q with a maximum capacity of μ to store the relative solution quality from PP+SIPPS and the MARL-planner (line 3). Subsequently, LNS2+RL counts the maximum length of individual paths in the initial solution (t_m), sets the timestep threshold t_l for pausing the MARL-planner, along with the maximum length t_h of each hybrid path, where the constant value $d_h > d_l$ (line 4). If the termination criteria are not met, LNS2+RL iteratively selects a subset of agents $A_s \subseteq A$ using the ALNS, and removes their paths $P^- = \{p_i \in P : a_i \in A_s\}$ from P , treating the remaining part of the path set $P \setminus P^-$ as fixed to construct a PMDO re-planning task (lines 6-7). The neighborhood size (the size of A_s) is fixed at 8 (equivalent to the number of agents used in MARL training) or 16. If the size of Q is below than μ , or its average exceeds another threshold ρ , LNS2+RL infers that the solution quality of the MARL-planner significantly exceeds that of PP+SIPPS at this stage (line 8). Therefore, LNS2+RL chooses the trained MARL-planner as the re-planning solver. The function in line 9 uses the MARL-planner to predict actions until timestep t_l (or until the re-planning task is fully resolved, i.e., all agents have reached their goal without future soft collisions). It yields two path sets: \hat{P} , derived by PP+SIPPS at the onset of the re-planning task, acting as the reference paths for the MARL policy, and path set P^{rl} , computed by the MARL policy. For incomplete paths in P^{rl} where agents haven't reached their goals, we employ PP+SIPPS to plan the remaining paths from t_l and merge these new paths with the existing ones (Line 10). Subsequently, all path lengths in P^{rl} are reviewed, and those exceeding t_h are directly replaced with paths re-planned by PP+SIPPS from timestep zero (lines 11). This operation aims to remove non-contributory segments planned by the MARL-planner, thus reducing the SoC of the final solution P and planning time for subsequent iterations. Next, LNS2+RL updates Q by appending 0 if $CP(P^{rl}) \geq CP(\hat{P})$, and 1 otherwise (lines 12). Finally, LNS2+RL first checks whether P^{rl} meets the update condition (line 13), namely if the CP of the repaired path set $(P \setminus P^-) \cup P^{rl}$ is no larger than that of the old path set. If not, LNS2+RL

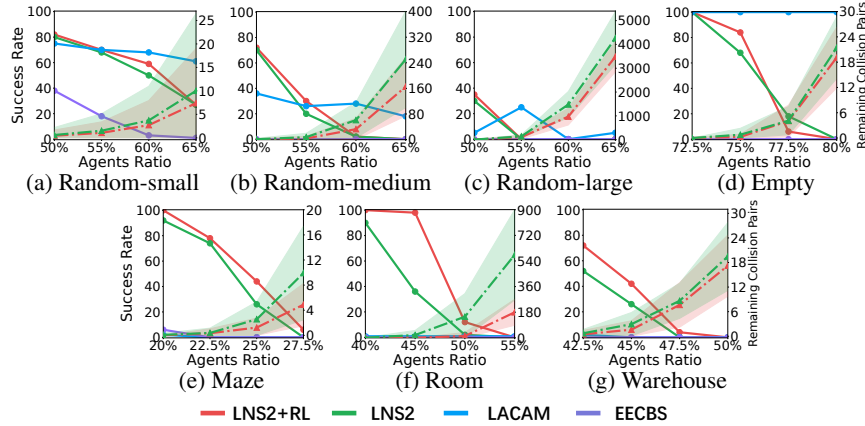


Figure 3: Result on different map types. The success rate is the percentage of tasks fully solved within the planning time constraints (i.e., where all agents reached their goal without collisions). The remaining collision pairs metric represents the number of CP remaining in the overall solution after reaching the time constraint and is only available for LNS2+RL and LNS2. The confidence interval (shaded area) represents one standard deviation of the remaining CP. All three random maps have a 17.5% obstacle density. Except for the random-small map with a size of 10×10 and the random-large map with a size of 50×50 , all other five maps have a size of 25×25 . For maps with sizes 10×10 , 25×25 , and 50×50 , the time constraints for each task are 100 seconds, 600 seconds, and 5000 seconds, respectively, with test counts of 100, 50, and 20. The neighborhood size of LNS2+RL is 16 on random-large maps and 8 on all other maps.

continues to check whether \hat{P} meets the update condition (line 22). The MARL-planner continues to re-plan until either the switching condition or termination condition is met. Once the re-planning solver switches to PP+SIPPS, it cannot switch back to the MARL-planner and always addresses remaining collisions using the same procedure as LNS2.

6 Experiments

We compare LNS2+RL with vanilla LNS2 Li et al. (2022) as well as a representative set of scalable high-quality MAPF algorithms: the bounded-suboptimal algorithm EECBS Li et al. (2021) (with a suboptimality factor $w = 5$), the complete but unbounded-suboptimal algorithm LACAM Okumura (2023), the MARL-based algorithm SCRIMP Wang et al. (2023), and the priority-based planner (PP) with random restarts (using SIPP Phillips & Likhachev (2011) to plan paths for single agents) Cohen et al. (2018). Here, we only show the results of LNS2, EECBS, and LACAM because the SR of SCRIMP and PP are 0% in most tasks, and they cannot solve even the simplest tasks in the random-small map. Both LNS2+RL and LNS2 use PP+SIPPS to find the initial solution and ALNS to generate neighborhoods. Code for LNS2, EECBS, LACAM was written in C++, and LNS2+RL was written in both C++ and Python and connected using pybind (**Our full training and testing code is available at** <https://github.com/marmotlab/LNS2-RL>). All experiments were conducted on a server equipped with one Nvidia GeForce RTX 3090 GPU and an AMD Ryzen 9 7950X3D 16-Core Processor. To obtain results faster, LNS2+RL, LNS2, EECBS used Ray to test multiple MAPF tasks simultaneously. However, due to high memory demands (we limited the maximum memory to 100GB per task), LACAM was tested using a single process.

6.1 Results for multiple map types

The evaluation results presented in Figure 3 demonstrate that LNS2+RL consistently achieves equal or higher SR compared to LNS2 across all tasks, except for those on the empty map with 77.5% agent density. It is noteworthy that the improvement of LNS2+RL on CP is more pronounced. In tasks with 65% agent density on the random-small map, despite both algorithms achieving the same SR, LNS2+RL remarkably reduces the remaining CP by 26.3% compared to LNS2.

The structural complexity of maps significantly influences algorithm performance. Despite being trained on random maps without prior exposure to highly structured environments like mazes, rooms, and warehouses, LNS2+RL demonstrates remarkable improvements in SR on these three types of maps. Conversely, LACAM excels on less structured maps, achieving a 100% SR on empty maps, but close to 0% SR on highly structured maps. EECBS consistently ranks as the poorest performing algorithm, with SR often remaining at 0% due to the high difficulty of the selected tasks.

Table 3: Comparing MARL policy against PP+SIPPS on low-level re-planning tasks of MAPF tasks on random-medium map with 65% agent density. The difference between collisions and CP is that for n collisions involving the same agents, the number of collisions is counted as n , but CP is counted as 1. The percentages in parentheses represent the performance ratio of the solution obtained by the MARL policy compared to that of PP+SIPPS.

Iterations	Collisions		Collision Pairs		Sum of Cost		Time	
	PP+SIPPS	MARL	PP+SIPPS	MARL	PP+SIPPS	MARL	PP+SIPPS	MARL
1	406.9	106.9(-73.7%)	109.9	93.9(-14.6%)	439.0	592.5(+35.0%)	0.012	0.153(+1175%)
50	471.5	129.9(-72.5%)	107.9	106.4(-1.2%)	564.1	675.3(+19.7%)	0.019	0.159(+737%)
100	488.3	130.8(-73.2%)	101.5	103.8(+2.3%)	597.2	689.9(+15.5%)	0.024	0.176(+633%)

Furthermore, taking the tasks in Table 2 as an example, the SoC for LNS2+RL only averages 1.03% higher than that of LNS2. Despite LACAM displaying higher SR on the random-small map, its SoC notably lags behind. Conversely, EECBS consistently achieves the best SoC but at the expense of obtaining the lowest SR. Moreover, LNS2+RL and LNS2 offer the added benefit of maintaining consistent memory usage, in contrast to LACAM and EECBS, whose memory usage escalates rapidly over time due to the generation of longer paths or larger search frontiers.

Table 2: Sum of costs on random-small map with 50%, 55%, 60%, 65% agent density (accounting only for successful tasks).

Algorithms	Sum of Cost			
	LNS2+RL	852.7	942.6	994.9
LNS2	831.0	939.4	972.4	1064.2
LACAM	2395.2	5288.3	5035.1	306438.3
EECBS	825.1	912.7	929.7	1030.0

6.2 Performance analysis

Table 3 compares the average performance of the MARL policy and PP+SIPPS in replanning tasks across different numbers of iterations. The MARL policy clearly produces fewer collisions overall, but its advantage in reducing CP is less pronounced, indicating that the MARL policy tends to cause collisions with different agents. With re-planning task difficulty decreasing as iterations increase, the MARL policy’s advantage in reducing CP diminishes. Given that the speed of the MARL policy is nearly seven times slower than that of PP+SIPPS, switching to PP+SIPPS becomes a necessary trade-off between time and solution quality.

Figure 4 illustrates the trend of the number of remaining CP over 2000 iterations in MAPF tasks on random-medium maps with a 65% agent density. As expected, in the early stage, before switching to PP+SIPPS, the number of CP for LNS2+RL decreases at a faster rate. After switching, the gap between LNS2+RL and LNS2 continues to widen, as the high solution quality achieved by the MARL policy reduces the difficulty of subsequent replanning tasks.

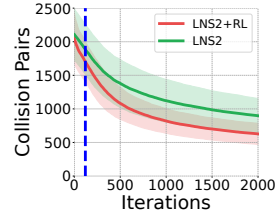


Figure 4: Number of remaining collision pairs through the iterative replanning process. The dashed blue line shows the switch from MARL to PP+SIPPS.

6.3 Real world experiment

As shown in Figure 1, we implemented our algorithm on a team of 90 virtual and 10 real robots in a warehouse environment. Since during the planning process, our algorithm assumes the position of all agents to be perfectly known at all times, we use ground truth positions for our virtual robots and use external localization (here, the *Optitrack Motion Capture System*) to obtain accurate position information for our real robots. However, the planned path may not be executed accurately due to disturbances and control inaccuracies. To eliminate these errors, we implement an *Action Dependency Graph* (ADG), as proposed by Höning et al. (2019). An ADG introduces a precedence order for the agents occupying a cell to ensure that errors in executing the planned path do not propagate and disrupt the overall execution plan. From our experiment, we observe that agents can reach their goals quickly without collisions, and errors are eliminated by the ADG, demonstrating the potential of using our method in the real world. More information about our experiment is included in Appendix A.4, and the full video is available in the supplementary material.

7 Conclusion

This paper introduces LNS2+RL, a novel MAPF algorithm that combines MARL with large neighborhood search. It follows the overall framework of LNS2, beginning with a path set that may contain collisions and then iteratively replanning paths for subsets of agents until the path set becomes collision-free. In early iterations, LNS2+RL addresses these challenging replanning tasks with a MARL-based planner, which offers higher solution quality but at a slower pace. As iterations progress, it adaptively switches to a fast, priority-based planner to quickly resolve remaining collisions. Our experiments on high-difficulty tasks across various world sizes, team sizes, and map structures

consistently demonstrate the superior performance of LNS2+RL compared to other SOTA MAPF algorithms. The practicality of LNS2+RL is validated in a hybrid warehouse mockup simulation involving 10 real-world and 90 simulated robots. However, the MARL planner we use still relies on paths computed by SIPPS, and its SoC cannot be guaranteed as optimal. Future work will explore how to improve this MARL-based planner.

References

- Barer, M., Sharon, G., Stern, R., and Felner, A. Suboptimal variants of the conflict-based search algorithm for the multi-agent pathfinding problem. In *Proceedings of the International Symposium on Combinatorial Search*, volume 5, pp. 19–27, 2014.
- Bengio, Y., Louradour, J., Collobert, R., and Weston, J. Curriculum learning. In *Proceedings of the 26th annual international conference on machine learning*, pp. 41–48, 2009.
- Bojarski, E., Felner, A., Stern, R., Sharon, G., Betzalel, O., Tolpin, D., and Shimony, E. Icbs: The improved conflict-based search algorithm for multi-agent pathfinding. In *Proceedings of the International Symposium on Combinatorial Search*, volume 6, pp. 223–225, 2015.
- Cohen, L., Koenig, S., Kumar, T. S., Wagner, G., Choset, H., Chan, D. M., and Sturtevant, N. R. Rapid randomized restarts for multi-agent path finding: Preliminary results. In *AAMAS*, pp. 1909–1911, 2018.
- Erdmann, M. and Lozano-Perez, T. On multiple moving objects. *Algorithmica*, 2:477–521, 1987.
- Goldenberg, M., Felner, A., Stern, R., Sharon, G., Sturtevant, N., Holte, R. C., and Schaeffer, J. Enhanced partial expansion a. *Journal of Artificial Intelligence Research*, 50:141–187, 2014.
- He, K., Zhang, X., Ren, S., and Sun, J. Deep residual learning for image recognition. In *Proceedings of the IEEE conference on computer vision and pattern recognition*, pp. 770–778, 2016.
- Hönig, W., Kiesel, S., Tinka, A., Durham, J. W., and Ayanian, N. Persistent and robust execution of mapf schedules in warehouses. *IEEE Robotics and Automation Letters*, 4(2):1125–1131, 2019.
- Huang, T., Li, J., Koenig, S., and Dilkina, B. Anytime multi-agent path finding via machine learning-guided large neighborhood search. In *Proceedings of the AAAI Conference on Artificial Intelligence*, volume 36, pp. 9368–9376, 2022.
- Li, J., Ruml, W., and Koenig, S. Eecbs: A bounded-suboptimal search for multi-agent path finding. In *Proceedings of the AAAI Conference on Artificial Intelligence*, volume 35, pp. 12353–12362, 2021.
- Li, J., Chen, Z., Harabor, D., Stuckey, P. J., and Koenig, S. Mapf-Ins2: Fast repairing for multi-agent path finding via large neighborhood search. In *Proceedings of the AAAI Conference on Artificial Intelligence*, volume 36, pp. 10256–10265, 2022.
- Luna, R. and Bekris, K. E. Push and swap: Fast cooperative path-finding with completeness guarantees. In *IJCAI*, pp. 294–300, 2011.
- Ma, Z., Luo, Y., and Ma, H. Distributed heuristic multi-agent path finding with communication. In *2021 IEEE International Conference on Robotics and Automation (ICRA)*, pp. 8699–8705. IEEE, 2021.
- Ng, A. Y., Harada, D., and Russell, S. Policy invariance under reward transformations: Theory and application to reward shaping. In *Icml*, volume 99, pp. 278–287. Citeseer, 1999.
- Okumura, K. Lacam: Search-based algorithm for quick multi-agent pathfinding. In *Proceedings of the AAAI Conference on Artificial Intelligence*, volume 37, pp. 11655–11662, 2023.
- Phillips, M. and Likhachev, M. Sipp: Safe interval path planning for dynamic environments. In *2011 IEEE international conference on robotics and automation*, pp. 5628–5635. IEEE, 2011.

- Sartoretti, G., Kerr, J., Shi, Y., Wagner, G., Kumar, T. S., Koenig, S., and Choset, H. Primal: Pathfinding via reinforcement and imitation multi-agent learning. *IEEE Robotics and Automation Letters*, 4(3):2378–2385, 2019.
- Schulman, J., Wolski, F., Dhariwal, P., Radford, A., and Klimov, O. Proximal policy optimization algorithms. *arXiv preprint arXiv:1707.06347*, 2017.
- Sharon, G., Stern, R., Felner, A., and Sturtevant, N. R. Conflict-based search for optimal multi-agent pathfinding. *Artificial Intelligence*, 219:40–66, 2015.
- Shi, X., Chen, Z., Wang, H., Yeung, D.-Y., Wong, W.-K., and Woo, W.-c. Convolutional lstm network: A machine learning approach for precipitation nowcasting. *Advances in neural information processing systems*, 28, 2015.
- Skrynnik, A., Andreychuk, A., Yakovlev, K., and Panov, A. I. When to switch: Planning and learning for partially observable multi-agent pathfinding. *IEEE Transactions on Neural Networks and Learning Systems*, 2023.
- Wagner, G. and Choset, H. M*: A complete multirobot path planning algorithm with performance bounds. In *2011 IEEE/RSJ international conference on intelligent robots and systems*, pp. 3260–3267. IEEE, 2011.
- Wagner, G. and Choset, H. Subdimensional expansion for multirobot path planning. *Artificial intelligence*, 219:1–24, 2015.
- Wang, B., Liu, Z., Li, Q., and Prorok, A. Mobile robot path planning in dynamic environments through globally guided reinforcement learning. *IEEE Robotics and Automation Letters*, 5(4): 6932–6939, 2020.
- Wang, Y., Xiang, B., Huang, S., and Sartoretti, G. Scrimp: Scalable communication for reinforcement- and imitation-learning-based multi-agent pathfinding. In *2023 IEEE/RSJ International Conference on Intelligent Robots and Systems (IROS)*, pp. 9301–9308. IEEE, 2023.

A Appendix

A.1 Additional results

A.1.1 Detailed results

The detailed results of Section 6.1 can be found in Table 4.

A.1.2 Results for different time limits and easier tasks

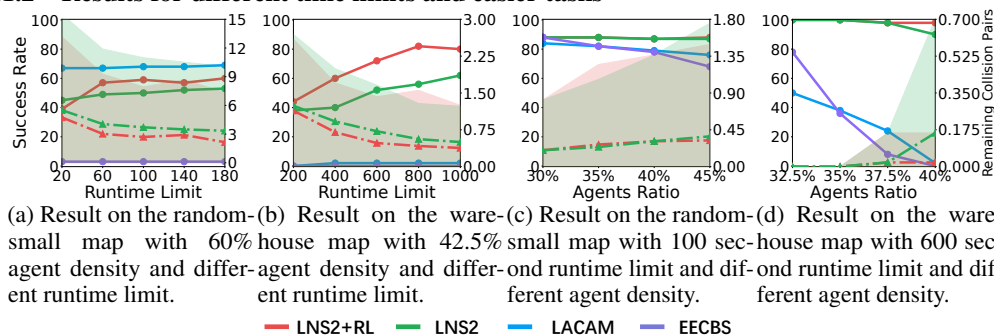


Figure 5: Result with different runtime limit and lower agent density.

In this section, we use the random-small map and warehouse map as representatives of less-structure maps and high-structure maps, respectively, to evaluate the performance of algorithms under varying runtime limits and task difficulties. Specifically, we conducted the runtime-limit experiments on the random-small map with a 60% agent density and the warehouse map with a 42.5% agent density. Their results are shown in Figure 5a and 5b. These results indicate that: First, the relative performance ranking of the algorithms remains consistent across different runtime limits, as discussed in the main

Table 4: Average performance along MAPF metrics of different algorithms for instances with different world sizes, team sizes, and map structure. For maps with sizes 10×10 , 25×25 , and 50×50 , the time constraints for each task are 100 seconds, 600 seconds, and 5000 seconds, respectively, with test counts of 100, 50, and 20. The success rate is the percentage of tasks fully solved within the planning time constraints (i.e., where all agents reached their goal without collisions). The sum of cost only accounts for successful tasks. Partial runtime data for LACAM is unavailable because some tasks in the test exceeded the maximum memory limit we set (100GB), leading to premature termination. The remaining collision pairs metric represents the number of CP remaining in the overall solution after reaching the time constraint and is only available for LNS2+RL and LNS2. Percentages in parentheses represent the reduced remaining CP ratio of LNS2+RL compared to LNS2. \uparrow indicates that “higher is better”, and \downarrow “lower is better”. “-” represents unavailable data. The results of the best-performing algorithms in each task are highlighted in bold.

Methods	Success Rate \uparrow		Sum of Cost \downarrow		Runtime \downarrow		Remaining Collisions Pairs \downarrow						
	Random-small: $10 * 10$ world size with 17.5% static obstacle rate and 50%, 55%, 60%, 65% agents density												
LNS2+RL	82%	70%	852.7	942.6	994.9	1052.8	21.6	34.9	49.8	79.9	0.45 (-25.0%)	2.70 (-27.2%)	7.44 (-25.7%)
LNS2	80%	68%	831.0	939.4	972.4	1064.2	20.8	33.9	54.1	77.0	0.60	1.51	3.71
EECBS	38%	18%	825.1	912.7	929.7	1030.0	63.9	82.8	97.1	99.1	-	-	-
LACAM	75%	68%	2395.2	5288.3	5035.1	306438.3	27.0	32.2	34.8	42.4	-	-	-
Random-medium: $25 * 25$ world size with 17.5% static obstacle rate and 50%, 55%, 60%, 65% agents density													
LNS2+RL	72%	30%	16726.3	16727.7	16605.0	-	222.1	486.8	593.5	600.0	0.80 (-20.0%)	3.54 (-53.2%)	32.52 (-46.5%)
LNS2	70%	20%	14157.5	15037.1	16513.0	-	256.8	509.8	591.7	600.0	1.00	7.56	60.82
EECBS	0%	0%	-	-	-	-	600.0	600.0	600.0	600.0	-	-	250.66
LACAM	36%	28%	35070.2	70508.0	66149.3	127656.0	397.4	-	-	-	-	-	-
Random-large: $50 * 50$ world size with 17.5% static obstacle rate and 50%, 55%, 60%, 65% agents density													
LNS2+RL	35%	0%	127514.3	-	-	-	4308.7	5000.0	5000.0	5000.0	2.95 (-42.7%)	108.30 (-21.2%)	968.85 (-35.1%)
LNS2	30%	0%	130756.5	-	-	-	4329.2	5000.0	5000.0	5000.0	5.15	137.45	1477.10
EECBS	0%	0%	-	-	-	-	5000.0	5000.0	5000.0	5000.0	-	-	4261.85
LACAM	5%	25%	204820.0	955662.6	-	474872.0	-	-	-	-	-	-	-
Empty: $25 * 25$ world size with 0% static obstacle rate and 72.5%, 75%, 77.5%, 80% agents density													
LNS2+RL	100%	84%	20155.2	20132.5	19278.0	-	94.7	333.5	596.6	600.0	0.00 (-0.0%)	0.26 (-66.7%)	4.04 (-11.0%)
LNS2	100%	68%	19365.8	19485.4	19390.4	-	117.7	403.8	575.5	600.0	0.00	0.78	4.12
EECBS	0%	0%	-	-	-	-	600.0	600.0	600.0	600.0	-	-	-
LACAM	100%	100%	24834.3	26929.9	29408.2	32298.9	0.006	0.007	0.007	0.008	-	-	-
Maze: $25 * 25$ world size with 45.76% static obstacle rate and 20%, 22.5%, 25%, 27.5% agents density													
LNS2+RL	100%	78%	5724.3	6523.3	7307.6	8698.0	16.4	183.6	416.0	568.8	0.00 (-100%)	0.34 (-10.5%)	1.24 (-51.6%)
LNS2	92%	74%	5563.3	6205.6	7210.6	-	67.6	217.9	493.5	600.0	0.08	0.38	2.56
EECBS	6%	0%	-	-	-	-	600.0	600.0	600.0	600.0	-	-	9.92
LACAM	2%	0%	41924.0	-	-	-	588.8	600.0	600.0	600.0	-	-	-
Room: $25 * 25$ world size with 19.52% static obstacle rate and 40%, 45%, 50%, 55% agents density													
LNS2+RL	100%	98%	35497.9	44779.1	58620.2	-	41.3	154.5	577.9	600.0	0.00 (-100%)	0.02 (-99.9%)	12.14 (-91.8%)
LNS2	90%	36%	26660.6	35221.3	39378.0	-	167.1	467.9	599.2	600.0	0.34	19.44	148.22
EECBS	0%	0%	-	-	-	-	600.0	600.0	600.0	600.0	-	-	582.5
LACAM	0%	0%	-	-	-	-	600.0	600.0	600.0	600.0	-	-	-
Warehouse: $25 * 25$ world size with 28.8% static obstacle rate and 42.5%, 45%, 47.5%, 50% agents density													
LNS2+RL	72%	42%	11202.9	12240.2	12082.0	-	296.9	458.9	595.6	600.0	0.48 (-33.3%)	1.60 (-45.6%)	17.22 (-23.8%)
LNS2	52%	26%	11027.3	11892.8	-	-	383.2	526.0	600.0	600.0	0.72	2.94	8.64
EECBS	0%	0%	-	-	-	-	600.0	600.0	600.0	600.0	-	-	-
LACAM	2%	0%	3061736.0	-	-	-	-	-	-	-	-	-	-

paper. LNS2+RL maintains its superiority over LNS2 in both SR and CP. Second, each algorithm has a distinct runtime limit threshold, beyond which its SR stabilizes. Notably, the thresholds of LNS2+RL and LNS2 exceed those of LACAM and EECBS. For instance, as depicted in Figure 5a, increasing the runtime limit from 20 to 60 seconds results in an 18% increase in SR for LNS2+RL and a 4% increase for LNS2, while the SRs for LACAM and EECBS remain unchanged.

Subsequently, we maintained a constant runtime limit while progressively reducing task difficulty (agent density). The results, illustrated in Figures 5c and 5d, indicate that: First, EECBS and LACAM perform relatively well on less challenging tasks, but the performance gaps between them and LNS2+RL and LNS2 widen as task difficulty escalates. Second, although in simpler tasks, the less pronounced advantages of the MARL-planner over PP+SIPPS lead to an earlier meeting of the switching condition, thus reducing the proportion of MARL-planner usage. However, LNS2+RL continues to achieve performance similar to that of LNS2.

A.1.3 Impact of different hyperparameters

Here, we take tasks on the random-small map with 60% agent density as an example to show the impact of the hyperparameters used to insert the MARL planner into the overall framework. These hyperparameters include the neighborhood size in MARL planning, the threshold ρ to switch the replanning solver from MARL planner to PP+SIPPS, the time step t_l to stop MARL planning, and the maximum length of the hybrid path t_h . The results are shown in Table 5 6 7 8. The hyperparameter values we selected outperformed others, yet the changes in hyperparameters did not exhibit a clear trend in SR. It’s worth noting that the optimal values for hyperparameters may vary across different tasks, necessitating fine-tuning to achieve the best performance of LNS2+RL. For instance, in handling challenging tasks, using larger neighborhood sizes and smaller switching thresholds can increase the proportion of paths computed by the MARL-planner, thereby further leveraging its advantages to improve SR.

Table 5: Success rate for different neighborhood sizes

Neighborhood Size	4	8	16
Success Rate	55%	59%	57%

Table 6: Success rate for different ρ

Switch Threshold ρ	0.2	0.25	0.3	0.35	0.4
Success Rate	58%	57%	59%	50%	56%

Table 7: Success rate for different t_l

Stop MARL planning t_l	0.8	1.2	1.6
Success Rate	55%	59%	58%

Table 8: Success rate for different t_h

Maximum Length t_h	1.8	2.2	2.6
Success Rate	57%	59%	54%

A.2 Map visualization

Figure 6 illustrates examples of the maps used for testing. In all maps, purple cells represent static obstacles, and yellow cells represent empty areas. The static obstacle layouts of the maze, room, and warehouse maps are fixed, and the obstacle layouts of the three random maps are randomly regenerated in each instance. For every instance of all maps, the agents’ distinct starting and goal positions are randomly chosen from empty cells within the same connected region of the map. The tasks tested in Section 6.1 are challenging, with the vacancy rates for the most difficult tasks on the seven maps only being 17.5%, 17.5%, 17.5%, 20%, 26.74%, 25.48%, and 21.2% respectively.

A.3 Hyperparameters

Table 9 shows the hyperparameters used to train the MARL model and implement the LNS2+RL algorithm evaluated in Section 6 of our paper. The first 29 hyperparameters are those used to train the MARL model, while the remaining hyperparameters are used to insert the MARL planner into the overall framework. There are three different task difficulties in the curriculum learning of training

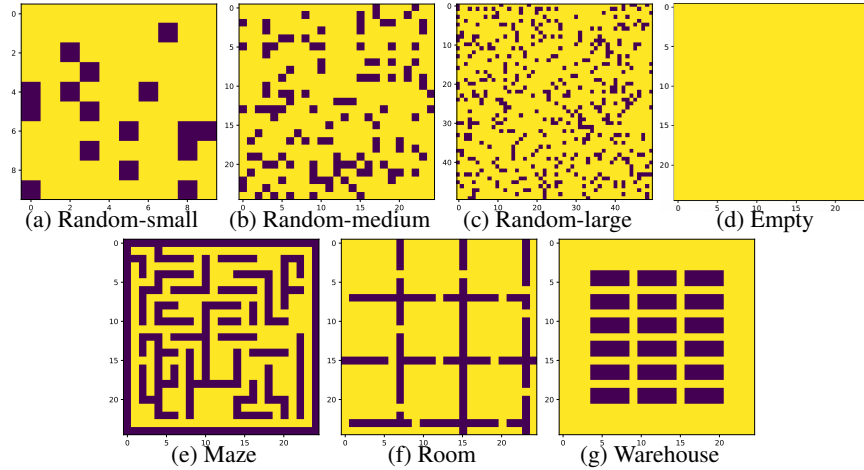


Figure 6: Visualized examples of the maps used for empirical evaluation.

Table 9: Hyperparameters table

Hyperparameter	Value
Number of MARL controlled agents	8
Ratio of total number of agents to world size	[(40%, 45%, 50%), (50%, 55%, 60%), (60%, 65%, 70%)]
World size	(10, 25, 50)
Obstacle density	[(5%, 7.5%, 10%), (10%, 12.5%, 15%), (15%, 17.5%, 20%)]
FOV size	9
Maximum episode length	356
α	(0.06, 0.05, 0.04)
β_t, β_h	2, 15
Reward shaping coefficient	0.2
$\delta, \delta_v, \delta_e$	10, 0.225, 0.075
Spatial and temporal coefficient for trajectory prediction	0.9, 0.1
Curriculum learning switching difficulty timestep	(1e7, 2e7)
Learning rate	1e-5
Discount factor	0.95
Gae lamda	0.95
Clip parameter for probability ratio	0.2
Gradient clip norm	50
Entropy coefficient ω_e	0.01
Actor loss coefficient ω_π	1
Critic loss coefficient ω_v	0.5
Invalid action loss coefficient $\omega_{invalid}$	0.5
Number of epoch	10
Number of processes	32
Mini batch size	512
Imitation learning timestep	(3e6, 2e6, 0)
Optimizer	AdamOptimizer
Training timestep for the first stage	7e6
Training timestep for the second stage	7e6
Maximum iterations	(30, 65, 100)
μ	20
ρ	0.3
d_t	1.2
d_h	2.2

stage one, so *ratio of total number of agents to world size*, *obstacle density*, α , *Imitation learning timestep* and *maximum iterations* contain three values/value sets, each value/value set corresponding to a task difficulty. The hyperparameters used in the second stage of training are mostly the same as those in the first stage of training, except *ratio of total number of agents to world size* = (60%, 65%, 70%), *obstacle density* = (15%, 17.5%, 20%), $\alpha = 0.04$, *maximum iterations* = 100

A.4 Real world experiment

A.4.1 Setup

We use a warehouse environment for our experiment (Figure 7). We assume that each pixel has a resolution of 0.5 m per grid unit, and based on this resolution, we realize a $7m \times 4.5m$ part of

the warehouse in the real world. We use a total of 100 robots for our experiment, of which 90 are virtual, and 10 are real *Sparklife Omnibots* robots with dimensions of approximately $0.3m \times 0.3m$ equipped with mecanum wheels for omnidirectional movement. We randomly generate the start and end positions of robots in the environment, with the constraint that the start and end positions of the real robots are in the real part of the warehouse. Since the MAPF problem assumes the accurate position of all agents for all time, we considered the ground truth positions for all virtual robots and used the *OptiTrack Motion Capture System* to get accurate positions for our real robots. Finally, we pre-plan the complete path set using LNS2+RL before actual execution and compute the joint actions agents should take at each timestep based on this path set.

A.4.2 Action dependency graph

The paths generated by LNS2+RL assume perfect operation for each agent at every step in the discrete map. However, due to the robots being imperfect and the environment being continuous, executing the planned path directly in the real world is infeasible. For instance, a planner may output a set of actions that lets an agent (say 'A') take another agent's (say 'B') position while Agent B moves to a new cell. If we were to try and execute this behavior on robots directly, a number of things, like errors in localization, delays in executing motor control commands, or differences in velocities, could lead to a collision between agents. To avoid such scenarios and make our joint set of actions executable, we follow the method proposed by Hönig et al. (2019) and construct an *Action Dependency Graph* (ADG). The main benefit of having an ADG is that it introduces a precedence order for the agents occupying a cell. This means that if an agent moves faster than the remaining agents, it will still wait for agents to catch up if it occupies a cell after another agent in the originally planned path. This behavior ensures that the errors in executing the planned path do not propagate and hamper the execution plan. Returning to our earlier example, using an ADG ensures that since Agent A is headed to a cell that Agent B occupies before it is in the originally planned path, it will wait for Agent B to reach a new cell before moving to occupy it.

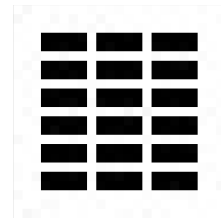


Figure 7: Map of the 23×23 warehouse environment used in our experiments, where black cells represent obstacles and white cells free space.

A.4.3 Execution

To implement the ADG, we first need to convert each action into a task that is to be executed by a robot. For this, we define a *Task* object as follows:

```
object Task {
  taskID; // Unique identifier for the task
  robotID; // Identifier for the robot which does this task
  action; // Action to be performed by the robot
  startPos; //start position of the robot before action execution
  endPos; // Position of the robot after action execution
  time; // Timestep when action to be executed
  status; // Marks if the task is staged, enqueued, or done
};
```

During execution, we first cycle through all agents, convert their actions into task objects, and use these tasks to construct an ADG. There are three statuses that an agent can have, namely: *STAGED*, *ENQUEUED* and *DONE*. All tasks are initialized with a *STAGED* status. The status is changed to *ENQUEUED* after all their dependent tasks in the ADG are done, meaning that this task is ready for execution. Lastly, the status is marked *DONE* when the agent reaches the *endPos* of the task.

A.4.4 ROS architecture

We have a *central node* that is responsible for generating and maintaining the ADG and distributing tasks for robots when they are to be enqueued. Furthermore, each robot has a *robot node*, which is responsible for receiving a task or set of tasks from the central node, extracting a goal from it, and using a PID controller to reach the goal. When a robot reaches its goal, it sends this information to

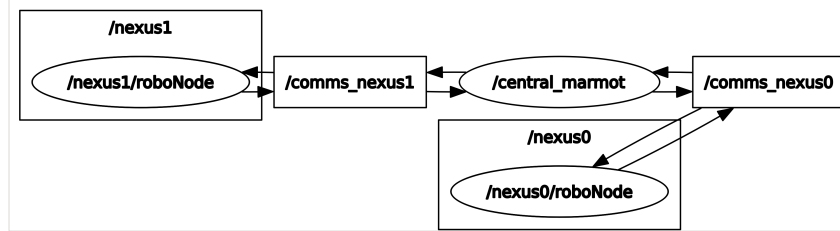


Figure 8: An RQT_Graph Snippet of our ROS architecture for 2 robots. Ovals indicate nodes, rectangles without ovals indicate topics, and rectangles with ovals indicate namespaces for multi-robots. The central_marmot node assigns tasks to robots (here nexus0 and nexus1) based on an *Action Dependency Graph*. Robots use those tasks to enqueue waypoints to the next goals. Upon reaching a goal, a robot will relay this information back to the central node.

the central node, marks this task as *DONE*, and uses the ADG to enqueue additional tasks. Figure 8 portrays a snippet of the architecture for 2 robots.